



Structural characterization and *in vivo* evaluation of retinyl palmitate in non-ionic lamellar liquid crystalline system

M. Chorilli^a, P.S. Prestes^b, R.B. Rigon^b, G.R. Leonardi^b, L.A. Chiavacci^a, V.H.V. Sarmiento^c, A.G. Oliveira^{a,*}, M.V. Scarpa^a

^a Departamento de Fármacos e Medicamentos, Faculdade de Ciências Farmacêuticas - UNESP, Rodovia Araraquara-Jaú, Km 01, 14.801-902, Araraquara, SP, Brazil

^b Curso de Farmácia, Faculdade de Ciências da Saúde - UNIMEP, Rodovia do Açúcar, Km 156, 13.400-911, Piracicaba, SP, Brazil

^c Centro de Ciências Exatas e Tecnologia, Departamento de Química - UFSE, Campus Alberto Carvalho, Av. Vereador Olímpio Grande s/n, 49.500-000, Itabaiana, SE, Brazil

ARTICLE INFO

Article history:

Received 8 November 2010

Received in revised form 17 February 2011

Accepted 19 February 2011

Available online 1 March 2011

Keywords:

Liquid crystalline systems

Retinyl palmitate

SAXS

Rheological analysis

In vivo effectiveness

ABSTRACT

Carrier systems for lipophilic drugs, such as the liquid crystalline systems (LCS) have been extensively studied to improve effect and selectivity. Retinyl palmitate (RP) is widely used in pharmaceutical and cosmetics products to improve the skin elasticity. The aim of this study was the development, characterization and the *in vivo* effectiveness of RP in non-ionic LCS structures. LCS containing polyether functional siloxane as oil phase, silicon glycol copolymer as surfactant and water in the ratio 30:10:60, with and without RP were studied. The results of the polarized light microscopy, small-angle X-ray scattering and rheology analysis indicated the presence of typical LCS structures with lamellar arrangement. Regardless of the presence of RP, the rheological studies showed the pseudo plastic behavior of the systems. However, highest hysteresis area was verified when comparing the system in the presence and in the absence of RP. Stability study SAXS monitored, carried out up to 30 days in various storage temperature conditions ($25 \pm 2^\circ\text{C}$, $37 \pm 2^\circ\text{C}$ and $5 \pm 2^\circ\text{C}$) demonstrated the great structural stability of the LCS systems. The *in vivo* effectiveness analysis suggests that the RP-loaded LCS provided a significant reduction of the orbicular wrinkles in human volunteers ($P=0.048$).

© 2011 Elsevier B.V. All rights reserved.

1. Introduction

Carrier systems for lipophilic drugs, such as the liquid crystalline systems (LCS) have been extensively studied to improve effect and selectivity [1–3]. It is known that the LCS can provide appropriated response for prolonged time, improving drug efficacy and reducing side effects [4–6]. These systems can be administered by different routes including ocular, oral, intraperitoneal, intramuscular, subcutaneous and cutaneous [7,8]. The development of new drug carrier systems based in the LCS structure has been a promising approach to increase and control the drug skin penetration [9–13]. Liquid crystalline phases are components mixtures that have mechanical properties of a liquid (fluidity) and optical characteristics of a crystal (optical anisotropy). Liquid crystalline systems are thermodynamically stable, thermotropic and lyotropic systems that can be stored for long periods without alterations [14–17]. Lyotropic liquid crystalline phases can be used as topical drug delivery systems because the high ability of drug solubilization, thermodynamic stability, a wide range of rheological properties and the high similarity

with the intercellular lipid membranes of the skin [18–21]. Swarbrick and Siverly investigated the topical application of vehicles containing LCS and established that the percutaneous absorption of lipophilic drug model decreases significantly when the proportion of liquid crystalline phases increases above 5–10% [22]. LCS can control drug release because the low interfacial tension arising at oil–water interface [23,24]. The mechanism involves the progressive diffusion into the skin and to systemic circulation [25–27]. They can bring a considerable increase in the solubility of poorly or water insoluble drugs [28–31].

Appropriated methods of investigation and characterization of LCS are often used in drug development. Sophisticated techniques such as polarized light microscopy (PLM), ionic conductivity, rheology and small-angle X-ray scattering (SAXS) are available to achieve this goal [32].

The use of silicones in topical formulations is a world trend, due to their advantages like non-comedogenicity, film formation, skin hydration, good skin feel and acceptance by the consumers. Thus, the association of LC and silicones allow for more stable and efficient formulations with adequate penetration, besides keeping the skin always moisturized [33,34].

Retinol, the form of vitamin A absorbed from animal food sources, is a yellow, fat-soluble substance. Since the pure alcohol form is unstable, the vitamin is found in tissues in a form of retinyl

* Corresponding author. Tel.: +55 1633016974; fax: +55 16 33220073.

E-mail addresses: oliveiag@fcar.unesp.br, ans-gomes@hotmail.com (A.G. Oliveira).

ester. It is also commercially produced and administered as esters such as retinyl acetate or palmitate and is widely used as active substance in pharmaceutical topical formulations. RP improves the elasticity of the skin reducing up to 10% [35–37].

The aim of this study was the development, characterization, and *in vivo* effectiveness determination of the LCS containing RP. For this RP-unloaded and RP-loaded LCS, obtained from the combination of polyether functional siloxane as oil phase, silicon glycol copolymer as surfactant and water were used.

2. Material and methods

2.1. Material

Polyether functional siloxane (PFS), DC[®] 5329 (S) and silicon glycol copolymer (SGC), DC[®] 193 (O) were purchased from Dow Corning (Michigan, USA), retinyl palmitate (RP) 1,000,000 UI/g from Roche (Greenzach, Germany). The high purity water (W) from Millipore Milli-Q plus purification system was used throughout.

2.2. Methods

2.2.1. Formulations preparation

The samples were prepared by heating the mixture of O and S to 45 °C. The W was heated up to 40 °C was then carefully added under gentle and constant stirring until the mixture reaches at room temperature. The obtained systems containing different proportions of the components were characterized in a pseudo-ternary phase diagrams in order to describe the proportions of the components to form lamellar liquid crystalline systems (LCS). The proportions of each component were calculated from titrations of the binary mixtures of oil phase and surfactant with water. The transitions from opaque semisolid phase to clear liquid system (CL), clear viscous system (CV), viscous translucent system (TV), liquid emulsion system (LEM), and viscous emulsion (VEM) and phase separation (PS) were delimited. The diagrams were obtained from the mixtures RP-loaded (1%) and RP-unloaded.

2.2.2. Polarized light microscopy

A drop of the sample was placed in a glass slide that was covered with a cover slip and then analyzed under polarized light. A Motic Type 102 M Optical Microscope equipped with a digital camera was used to analyze several fields of each sample at room temperature. The isotropic or anisotropic behavior of the samples was noted. Photomicrographs were taken at 200× magnification.

2.2.3. Small-angle x-ray scattering (SAXS)

The nanometric structure of the phases was studied by (SAXS) measurements. Data was collected at the Synchrotron SAXS beam line of the National Laboratory of Synchrotron Light (LNLS, Campinas, Brazil), equipped with an asymmetrically cut and bent Si (1 1 1) monochromator ($\lambda = 1.608 \text{ \AA}$) that yields a horizontally focused beam. A vertical position-sensitive X-ray detector and a multichannel analyzer were used to record the SAXS intensity, $I(q)$, as a function of the modulus of the scattering vector q , $q = (4\pi/\lambda)\sin(\varepsilon/2)$, ε being the scattering angle. The parasitic scattering produced by slits was subtracted from the total scattering intensity.

2.2.4. Rheological analysis

The rheological analysis of formulations was carried out with a controlled-stress Carrimed CSL 100 rheometer (TA instruments) with plate–plate geometry. This geometry consists of two stainless steel plates of 2 cm diameter with a gap of 200 μm between the plates. Samples were carefully applied to the lower plate, ensuring

that formulation shearing was minimized, and allowed to equilibrate for at least 3 min prior to analysis. The experiments were carried out with shear rates ($\dot{\gamma}$) in the range of 0.001–30 s^{-1} . The shear rate region used was selected on the basis of the strength of resistance to the applied stresses. The rheological measurements were performed on both the up and down curves. The data from the shear cycle were fitted to a power-law model, using Rheology Solutions Software (version Data V1.1.7, TA Instruments). All rheological determinations were carried out on all samples, at $25.0 \pm 0.2 \text{ }^\circ\text{C}$.

2.2.5. Wrinkles traces evaluation on the facial skin of human volunteers

This study was approved by the Research Ethics Committee of the Methodist University of Piracicaba, protocol 073/2005. The study was conducted on healthy women with white skin or light brown, aged between 30 and 45 years and with facial skin aging. It was selected 30 volunteers who did not use medicines for chronic use, except contraceptives, which were divided into three groups, each with ten volunteers. All volunteers were instructed to avoid the sun during the treatment period and guided to suspend the use of any product in the eyes periorbicular region one month before the beginning of the treatment. Terms of free consent were obtained from patients, who voluntarily participated after acknowledging the procedures of the study.

The first group used F1RP-unloaded to test de vehicle system, the second used F1 RP-loaded and the third was the control group (C) which did not use formulation. The volunteers were guided to apply fixed amount of the formulations 1×/day, at night, up to 30 days on the face skin including the eyelid region, through circular movements for 15 s. The entire volunteer's skin was previously photographed, using a CCD color microscope, Scope model. Reevaluation was carried out 30 days after the treatments.

For the calculation of the areas percentage with traces of wrinkles, the photographs were transferred to Corel Photo-Paint 8 software, the images divided in 266 areas of 1.2 cm^2 , in images with 10× of magnification. The area with traces of wrinkles of the eye orbit region of each volunteer was calculated by planimetry for point's counting. [38] For the effectiveness study, comparisons between the treatment groups were performed using the analysis of variance followed Tukey test. The analysis was considered statistically significant for $P < 0.05$.

3. Results and discussion

The data of the pseudo-ternary phase diagram shows that it is possible to add a great volume of oil phase and limited volume of water phase maintaining the thermodynamic stability of systems. Clear and translucent regions are obtained in a wide range region of the pseudo-ternary phase diagram (Fig. 1). The analysis of the phase diagram regions in Fig. 1 shows a distinct transition from LCS to VEM, TV and CL; and from LEM, LCS and CL to PS. Independently on the proportions of the S and O a complete clear liquid phase (CL) exists with the aqueous phase proportions up to 70%, but with wide field in the low aqueous phase proportion and high oil phase contents. In the region where aqueous phase predominates and up to about 30% of the oil a phase separation region followed by LEM, VEM, LCS region and a CL system were observed with a progressive increase in the surfactant proportion. The formation of CL was favored in the region of oil phase dominance, but phase separation was verified when the aqueous phase was predominant. Two LCS regions separated by a translucent region (TV) were also found. The first region has been described in high surfactant proportions (above 50%), low proportions of aqueous (between 20 and 40%) and oil phases (up to 25%); and one second

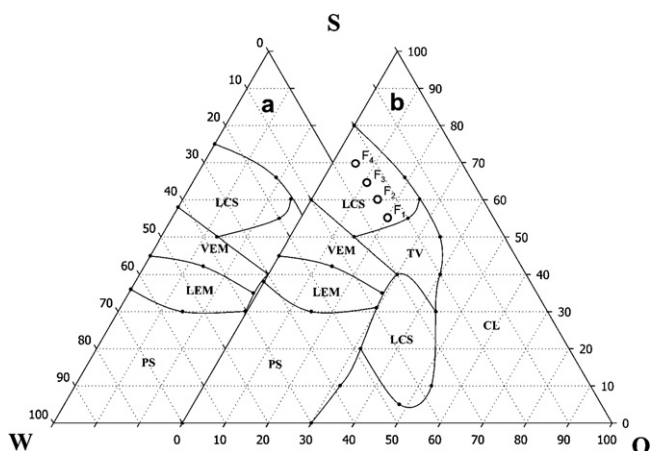


Fig. 1. Pseudo-ternary phase diagram for systems containing PFS (S), SGC (O) and purified water (W). Key: (a) Unloaded-system; (b) loaded system; (CL) clear liquid system; (LCS) liquid crystalline system; (TV) translucent viscous system; (VEM) viscous emulsion; (LEM) liquid emulsion; (PS) phase separation; (○) specific compositions of the studied systems, 25 °C.

region defined in low surfactant proportions (up to 40%), aqueous phase contents between 29 and 49%, and larger oil phase proportion (between 30 and 55%). Thus, this phenomenon is dependent on the O/S ratio and can be understood because when the oil phase proportion increased, the system went through a translucent intermediate phase which clearly indicates a transition region between the two LCS phases (Fig. 1).

We have found that in the interest LCS region, with high surfactant contents, the incorporation of the RP did not change significantly the domain regions of the phase diagram (Fig. 1). The systems remain isotropic, optically transparent and there were no sedimentation or phase separation after centrifugation 30,000 rpm for 30 min. The studied formulations are shown in Table 1 and the specific compositions were represented in the pseudo ternary phase diagram (Fig. 1). The formulations of Table 1 were obtained by varying the amounts of oil phase and surfactant in order to obtain different O/S ratios.

Table 1
Selected formulations for this study.

Components	F ₁ (%)	F ₂ (%)	F ₃ (%)	F ₄ (%)
Polyether functional siloxane (S)	55.0	60.0	65.0	70.0
Silicon glycol copolymer (O)	20.0	15.0	10.0	5.0
Water (W)	25.0	25.0	25.0	25.0
O/S ratio	0.36	0.25	0.15	0.075

Isotropic and anisotropic materials can be distinguished by polarized light microscopy. The optical properties of anisotropy can provide information on the structure and composition of materials such as lipid vesicles, microemulsions and liquid crystalline systems. Since the isotropic materials have only one refractive index and no restriction on the vibration plane of light passing through them so they have the same optical properties in all directions. Then, under polarized light isotropic materials are characterized by a dark field. Moreover, anisotropic material have optical properties that change with the orientation of the incident light in relation to crystallographic axes showing different refractive indices depending of the direction of propagation of light through the system and on the orientation of the vibration plane. Then, due to its molecular organization, the anisotropic liquid crystalline systems are birefringent and display Malta crosses under polarized light [39].

The photomicrographs of the RP-unloaded and RP-loaded formulations, analyzed by polarized light microscopy are shown in Figs. 2 and 3. For all samples the presence of Malta crosses was observed, which is characteristic of the structures of liquid crystalline phases [40]. This organization seems to be dependent on the O/S ratio [Table 1, Fig. 2F₁–F₄]. Thus, there are a large number of structures in Malta crosses at high O/S ratio, which sharply decreases with decreasing O/S ratio (Fig. 2F₁–F₄).

When the RP was incorporated into the system, a small decrease in the well-defined Malta crosses was also observed (Fig. 3F₁–F₄) demonstrating the low RP influence on the structural organization of the system (Figs. 2 and 3). In fact, it is well known that the appropriate combination between the oil phase, surfactant and water phase is the key for lamellar liquid crystalline systems formation [41]. However it is unclear whether Malta crosses are present or not in the photomicrographs of the systems at low O/S ratios. On the

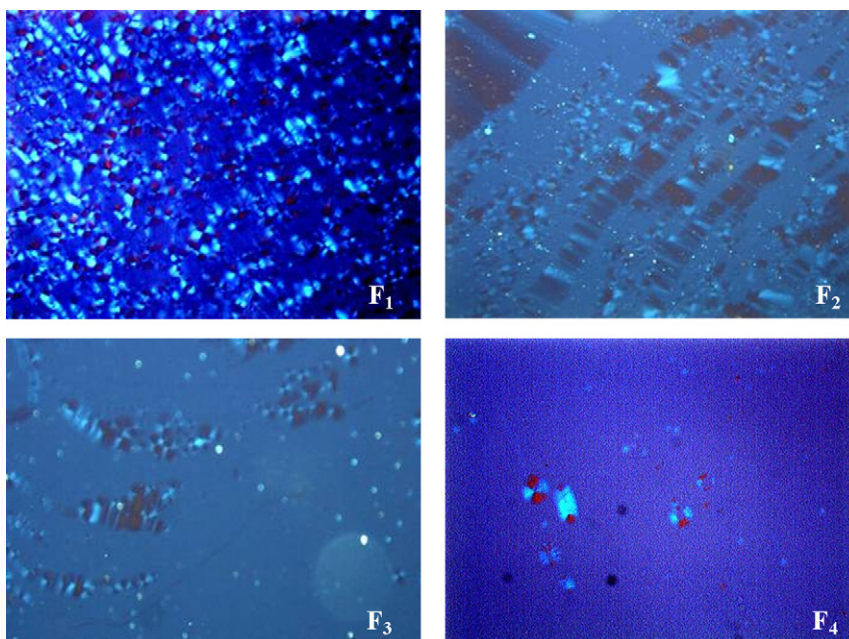


Fig. 2. Polarized light microscopy photomicrographs of the recently prepared RP-unloaded formulations (F₁–F₄) from LCS region of the phase diagram.

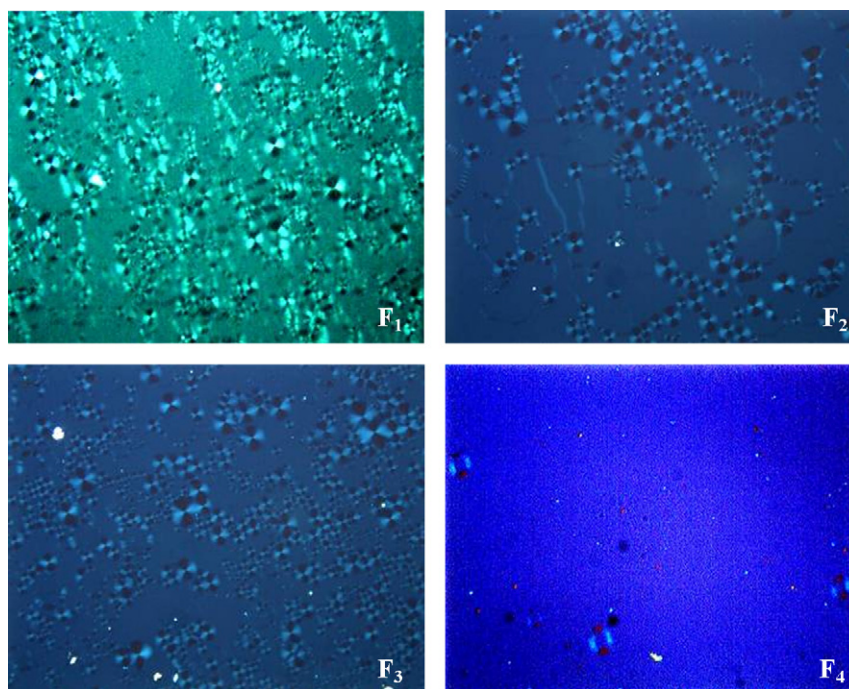


Fig. 3. Polarized light microscopy photomicrographs of the recently prepared RP-loaded formulations (F₁–F₄) from LCS region of the phase diagram.

other hand, it is also known that spherical structures formed by lipid bilayers such as liposomes exhibit Malta crosses in polarized light microscopy [42,43]. Thus, it may be likely that such condition the disintegration of the initial system occur, leading to the formation of fragments of crystalline liquid phases shown in photomicrographs 2C and 3C. These results are in agreement with the analysis of the SAXS data presented in Fig. 4, demonstrating the structural organization of lamellar phase of the system.

Other published studies also suggest that lamellar liquid crystalline phases are related to system stabilization due that the lamellar structure forms a shield around the globules, preventing the adhesion between then or the phase separation [44–47].

Further SAXS studies were performed in order to confirm the lamellar structure of the samples was performed and the intensity of the scattering patterns (I) were plotted versus the scattering vector modulus q (\AA^{-1}). For both RP-unloaded and RP-loaded LCS the curves of the SAXS data are shown in Fig. 4A and B, respectively.

It is well known that LCS can be oriented to form one, two or three-dimensional structures and the SAXS curves show Bragg peak intensities for specific values of the scattering vector q [48,49]. The relationship between the positions of these peaks on the q -axis discloses the crystalline structure type and allows that the structural parameters are calculated [50]. The d parameter was calculated by $d = 2\pi/q_m$, where q_{max} is the maximum intensity value of the scattering vector peak. For a lamellar liquid crystalline structure the relationship between the calculated correlation distances for each Bragg peak follows the relationship 1:2:3 [51]. From the data of Fig. 4A and B for all samples it was found the presence of two Bragg peaks with correlation distances of 1:2 which is indicative of the presence of a 1D lamellar structure, as shown in the PLM data in Figs. 2 and 3.

Regardless of the presence of RP, the SAXS patterns show a broad and intense peak, characteristic of lamellar liquid crystalline structure with strong spatial ordering. This feature was confirmed by the presence of large amounts of Maltese crosses (Figs. 2 and 3). Although the analysis by PLM shows a clear decrease in the amount of the Malta crosses by the increase in the O/S ratios, this structural difference could not be demonstrate through the SAXS analysis.

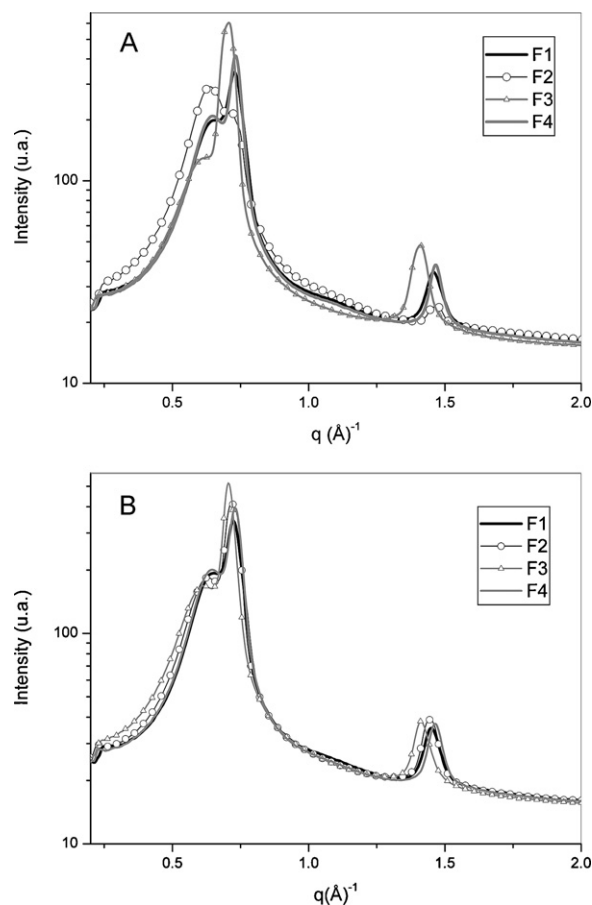


Fig. 4. SAXS analysis of F₁–F₄ formulations from CV region of the phase diagram. Key: (A) RP-unloaded LCS; (B) RP-loaded LCS.

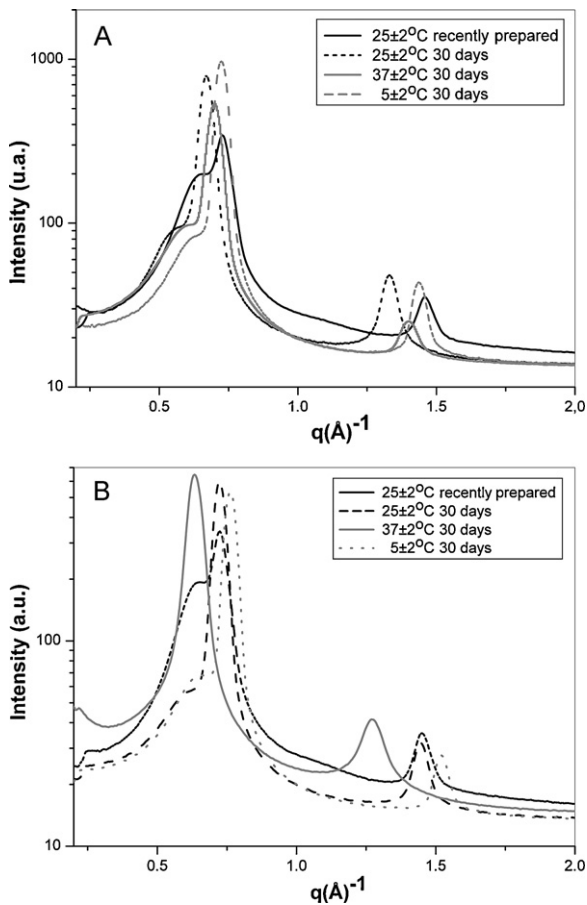


Fig. 5. SAXS analysis of F₁ formulation from CV region of the phase diagram at different temperatures. Key: (A) RP-unloaded LCS; (B) RP-loaded LCS.

Moreover, it was demonstrated that the incorporation of RP in the LCS systems induced no effect on the structural organization.

The RP-loaded and RP-unloaded formulations (Table 1) from LCS area of the pseudo ternary phase diagram (Fig. 1) were also used to stability study of the organized structures in different experimental conditions. For both F₁-unloaded and F₁-loaded RP, the SAXS curves obtained after 24 h of preparation at 25 °C were compared with the SAX data of the formulations after 30 days at 25, 37 and 5 °C. The results are shown in Fig. 5. Independently on the temperature of the storage time, the profile of the SAXS curves for all formulation showed two well defined peaks with correlation distances 1:2 demonstrating that the lamellar phase structure remains organized yet.

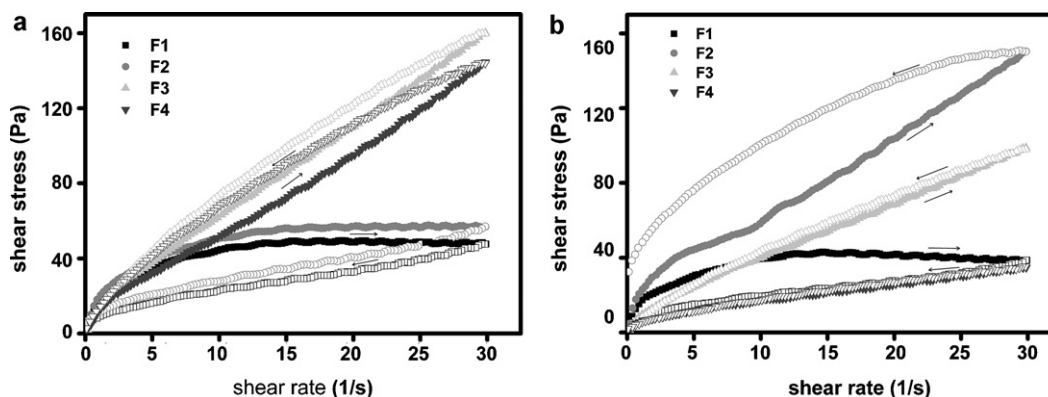


Fig. 6. Rheological behavior of F₁–F₄ formulations from CV region of the phase diagram (see Table 1 for formulations details). Key: (a) RP-unloaded LCS; (b) RP-loaded LCS.

For both RP-unloaded and RP-loaded the flow properties of the formulations from LCS region of the phases diagram are shown in Fig. 6. The non-linearity data from the shear rate and shear stress parameters explains the non-Newtonian pseudo-plastic fluid profile of the samples. This behavior is due to a lack in the internal organization of the system with the shear rate variation. These results reveal the presence of a structured network formed from the interaction between the formulation components, which is gradually broken with increasing shear stress. Then the internal resistance of the system structure decreases, causing a viscosity reduction [52].

Thus, after applying the tension the formulation showed smooth flow, leading to a great dispersion during the application and the formation of uniform film on the skin surface [53].

The liquid crystalline systems present high viscosity and the lamellar phase shows pseudo-plastic characteristic [54]. Pseudo plastic systems exhibit shear thinning without the initial resistance to deformation (yield stress) and can present the thixotropic phenomenon. In general materials with thixotropic characteristics show a strong ability to recovery its structure when the stress is removed. This phenomenon can be observed by the flow test, which the shear rate increases continuously with time from zero to maximum value and subsequently decreasing to zero in the same way [55]. For materials with thixotropic characteristics the results of the shear rate against shear stress curve generally include an ascending curve upward shifted in relation to downward curve as shown in Fig. 6.

The formation of organized structures like those shown in Fig. 6, which can disrupt under the effect of shear stress and rebuild it when the pressure is removed, is the main mechanism for material thixotropy. This phenomenon is a desirable characteristic in pharmaceutical dispersions, because the decrease in the viscosity (shear-thinning) facilitates the product application, while the time-dependent structure recovery after administration allows an efficient bioadhesion [54,56]. The obtained results also show that the presence of RP did not change the rheological profile of the studied formulations.

Moreover, another important approach is that the RP incorporation modified the hysteresis area of the systems (Fig. 7a–d). The F₁ RP-loaded stored at 37 ± 2 °C (Fig. 7c), showed a lower hysteresis area when compared with the F₁ RP-unloaded formulation. This phenomenon may be related to an increased stability of the system caused by the RP presence, which reduces the structural disorganization of the system by the effect of the shear stress.

The biological efficiency of the formulations was tested from the analysis of the photographs of the orbicular region of volunteer's eyes, recorded before (T_0) and after (T_{30}) treatment. The results are shown in Fig. 8 and express the percentage areas with wrin-

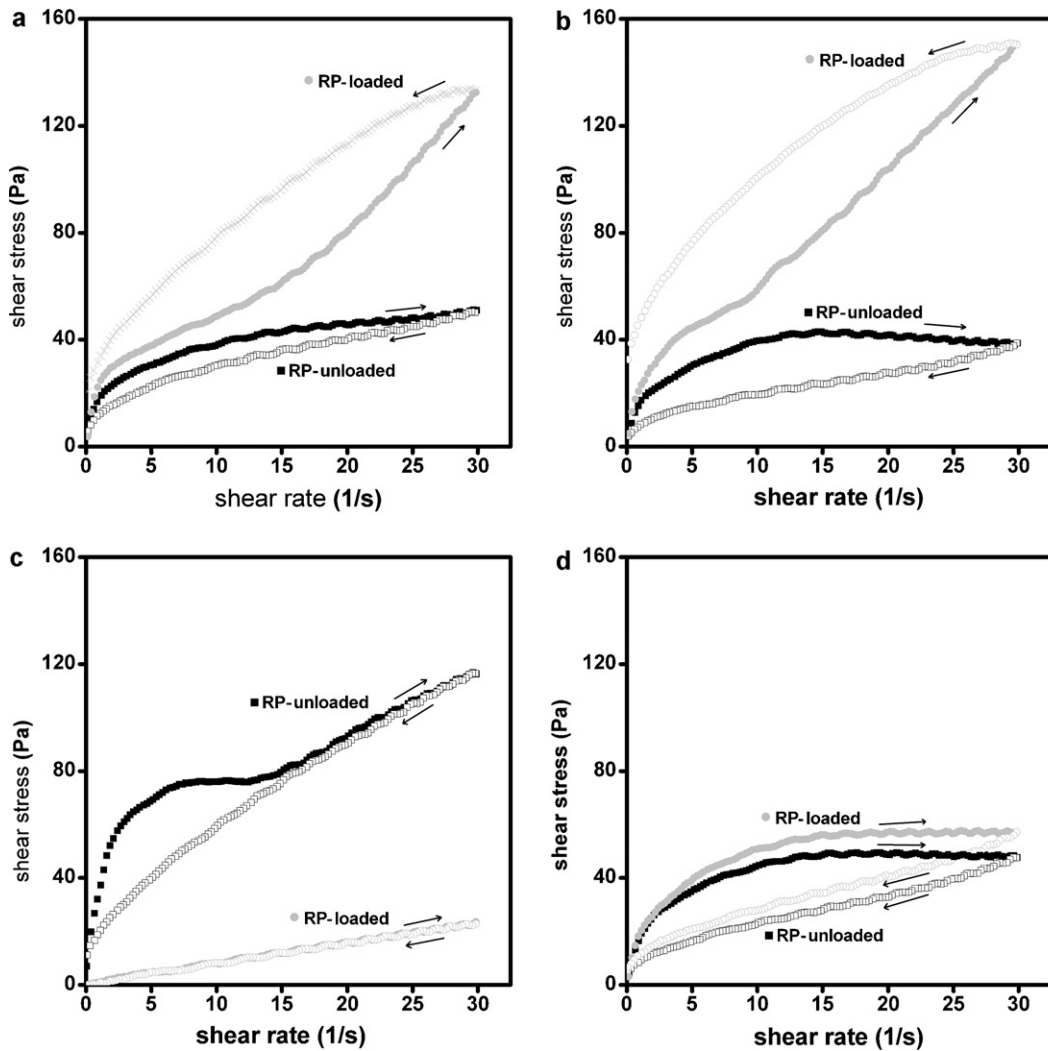


Fig. 7. Rheological behavior of the F₁ formulations from CV region of phase diagram (see Table 1 for formulations details). Key: (a) recently prepared at 25 ± 2 °C; (b) after 30 days storage at 25 ± 2 °C; (c) after 30 days of storage at 37 ± 2 °C; (d) after 30 days of storage at 5 ± 2 °C.

kles traces. The experimental data were submitted to the variance analysis according Tukey Test.

The group that received only the application of the empty LCS formulation during the 30 days of treatment showed no sta-

tistically significant difference ($P=0.09$) from the control group. However the application of the RP-loaded LCS formulation provided the reduction of the orbicular wrinkles from volunteers ($P=0.045$).

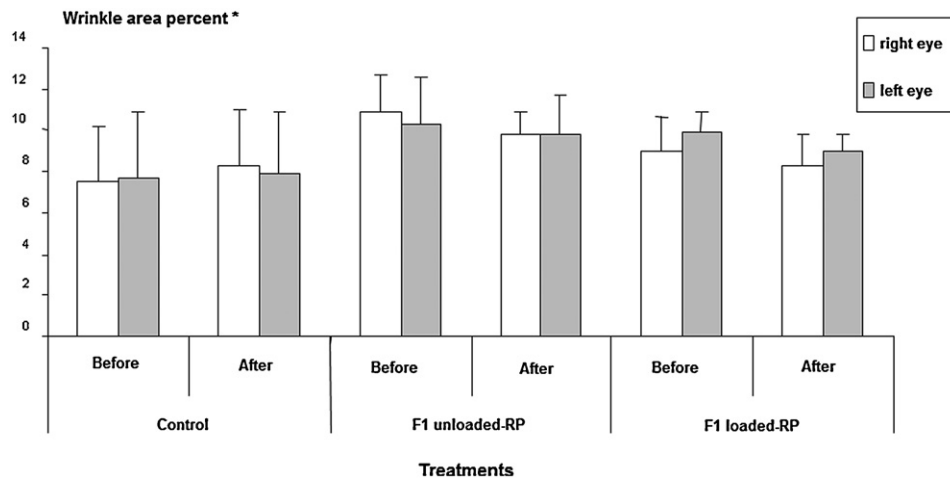


Fig. 8. Percentage of wrinkles traces in volunteers before and after treatment with F₁ formulation. *Measured from 1.2 cm² using images with 10× magnification. Mean ± SD from 10 volunteers.

The effect of the F1 RP-loaded formulation on the wrinkles, up to 30 days treatment, can be due to a controlled release with increase in the vitamin effect on the skin when the lamellar liquid crystalline system is present. It is well known that this compound is able to prevent some degenerative changes associated with aging skin such as dry skin and wrinkles [57,58]. In fact, other studies have reported increased effectiveness of drugs incorporated in LCS and related structures were described. The increase in the cutaneous moisturizing by diclofenac diethylamine in lamellar structures was previously observed [59]. The enhancement of the cutaneous permeability and anti-inflammatory effect of aceclofenac in microemulsions to treat muscular pains was also reported [60]. Spiclin and collaborators also verified an increase in the effectiveness of sodium ascorbyl phosphate by topical microemulsions [61]. A marked reduction in wrinkles with improved texture and elasticity of skin due to application of RP-based cosmetic formulations was related with the stratum corneum compression [62].

4. Conclusions

The studied systems containing Polyether functional siloxane, Polyether functional siloxane and water in its composition were able to form lamellar liquid crystalline phases. The systems were properly characterized by PLM and SAXS analysis. The rheological study showed that the formulations behave a non-Newtonian fluid, with characteristic of the pseudo-plastic material. The stability studies revealed that the presence of RP did not cause significant structural changes in the system. The incorporation of RP within LCS phases provided a significant reduction in the orbicular wrinkles in human's volunteers. Considering the field of control of the technology involved in the preparation of the system, the stability and the effectiveness response of the RP-loaded formulation, the carrier system may be a promising approach for RP delivery and a suitable vehicle for pharmaceutical and cosmetic applications.

Acknowledgements

The authors wish to thank FAPESP, CNPq and CAPES for the financial support.

References

- [1] G.M. Barratt, *Pharm. Sci. Technol. Today* 3 (2000) 163.
- [2] P. Couvreur, G. Barrat, E. Fattal, P. Legrand, C. Vauthier, *Crit. Rev. Ther. Drug Carrier Syst.* 19 (2002) 99.
- [3] A.G. Oliveira, L.A. Chiavacci, M.V. Scarpa, E.S.T. Egitto, in: L. Songjun (Ed.), *Current Focus on Colloids and Surfaces*, Transworld Research, Kerala, 2009.
- [4] M. Yokoyama, T. Okano, *Adv. Drug Deliv. Rev.* 21 (1996) 77.
- [5] M.A. Corrêa, M.V. Scarpa, M.C. Franzini, A.G. Oliveira, *Colloids Surf. B* 43 (2005) 112.
- [6] C. Vauthier, C. Dubernet, E. Fattal, H. Pinto-Alphandary, P. Couvreur, *Adv. Drug Deliv. Rev.* 55 (2003) 519.
- [7] K. Park, C. Kim, *Int. J. Pharm.* 181 (1999) 173.
- [8] T.P. Formariz, L.A. Chiavacci, V.H.S. Sarmiento, C.M. Franzini, A.A. Silva-Júnior, M.V. Scarpa, C.V. Santilli, E.S.T. Egitto, A.G. Oliveira, *Colloids Surf. B* 63 (2008) 295.
- [9] H. Lbouthoune, J. Chaulet, C. Ploton, F. Falson, F. Pirot, *J. Control. Release* 82 (2002) 319.
- [10] R.H. Müller, M. Radtke, S.A. Wissing, *Adv. Drug Deliv. Rev.* 54 (2002) S131.
- [11] R. Alvarez-Román, A. Naik, Y.N. Kalia, R.H. Guy, H. Fessi, *J. Control. Release* 99 (2004) 53.
- [12] R. Alvarez-Román, A. Naik, Y.N. Kalia, R.H. Guy, H. Fessi, *Pharm. Res.* 21 (2004) 1818.
- [13] K. Bouchemal, S. Briançon, E. Perrier, H. Fessi, I. Bonnet, N. Zydowicz, *Int. J. Pharm.* 269 (2004) 89.
- [14] T.P. Formariz, L.A. Chiavacci, M.V. Scarpa, A.A. Silva-Junior, E.S.T. Egitto, C.H.B. Terrugi, C.M. Franzini, V.H.V. Sarmiento, A.G. Oliveira, *Colloids Surf. B* 77 (2010) 47.
- [15] T.P. Formariz, V.H.V. Sarmiento, A.A. Silva-Junior, M.V. Scarpa, C.V. Santilli, A.G. Oliveira, *Colloids Surf. B* 51 (2006) 61.
- [16] K.C. Pestana, T.P. Formariz, C.M. Franzini, V.H.V. Sarmiento, L.A. Chiavacci, M.V. Scarpa, E.S.T. Egitto, A.G. Oliveira, *Colloids Surf. B* 62 (2008) 253.
- [17] T.P. Formariz, L.A. Chiavacci, V.H.V. Sarmiento, C.V. Santilli, E.S.T. Egitto, A.G. Oliveira, *Colloids Surf. B* 60 (2007) 28.
- [18] S.P. Vyas, V. Jaitely, P. Kanaujia, *Pharmazie* 52 (1997) 259.
- [19] A.C. Sintov, L. Shapiro, *J. Control. Release* 95 (2004) 173.
- [20] L. Sagalowicz, R. Mezzenga, M.E. Leser, *Curr. Opin. Colloid Interface Sci.* 11 (2006) 224.
- [21] Y. Ding, L. Chen, R. Guo, *Colloids Surf. A: Physicochem. Eng. Aspects* 295 (2007) 85.
- [22] J. Swarbrick, J.R. Siverly, *Pharm. Res.* 12 (1992) 1550.
- [23] W. Benton, *J. Dispersion Sci. Technol.* 3 (1982) 1.
- [24] T. Suzuki, H. Takei, S. Yamazaki, *J. Colloid Interface Sci.* 129 (1989) 491.
- [25] J. Ziegenmeyer, The influence of the vehicle on the absorption and permeation of drugs, in: R. Brandau, B.H. Lippold (Eds.), *Dermal and Transdermal Absorption*, Wissenschaftliche Verlagsgesellschaft mbH, Stuttgart, 1982.
- [26] H.E. Boddé, T. De Vringer, H.E. Junginger, *Prog. Colloid Polym. Sci.* 72 (1986) 37.
- [27] B. Berner, E.R. Cooper, Models of skin permeability, in: A.F. Kydonieus, B. Berner (Eds.), *Transdermal Delivery of Drugs*, vol. II, CRC Press, Boca Raton, 1987.
- [28] P.H. Elworthy, A.T. Florence, C.B. Macfarlane, *Solubilization by Surface Active Agents*, Chapman & Hall, London, 1986.
- [29] K. Kriwet, C.C. Müller-Goymann, *Eur. J. Biopharm.* 39 (1993) 234.
- [30] S. Engström, *Eur. J. Pharm. Sci.* 8 (1999) 243.
- [31] I. Csóka, E. Csanyi, G. Zapantis, E. Nagy, A. Fehér-Kiss, G. Horváth, G. Blazsó, I. Erős, *Int. J. Pharm.* 291 (2005) 11.
- [32] C.C. Müller-Goymann, *Eur. J. Pharm. Biopharm.* 58 (2004) 343.
- [33] M. Chorilli, P.S. Prestes, R.B. Rigon, G.R. Leonardi, M.V. Scarpa, *Química Nova* 32 (2009) 1036.
- [34] P.S. Prestes, M. Chorilli, L.A. Chiavacci, M.V. Scarpa, G.R. Leonardi, *J. Dispersion Sci. Technol.* 31 (2010) 117.
- [35] B. Idson, *Drug Cosmet. Ind.* 146 (1990) 26.
- [36] FDA (U.S. Food and Drug Administration), The U.S. Food and Drug Administration's Voluntary Cosmetics Registration Program, www.fda.gov, 2004.
- [37] N. Mei, Q. Xia, L. Che, M.M. Moore, P.P. Fu, T. Chen, *Toxicol. Sci.* 88 (2005) 142.
- [38] C.A. Mandarim-de-Lacerda, *Manual de quantificação morfológica: morfometria, alometria e astereologia*, CEBIO, Rio de Janeiro, 1994.
- [39] S.T. Hyde, *Handbook of Applied Surface and Colloid Chemistry*, John Wiley & Sons, New York, 2001.
- [40] I.A. Raman, H. Suhaimi, G.J.T. Tiddy, *Adv. Colloid Interface Sci.* 106 (2003) 109.
- [41] M. Rosoff, *Controlled Release of Drugs: Polymers and Aggregate Systems*, VCH Publishing, New York, 1989.
- [42] S. Chatterjee, D.K. Banerjee, Preparation, isolation, and characterization of liposomes containing natural and synthetic lipids, in: S.C. Basu, M. Basu (Eds.), *Liposome Methods and Protocols*, vol. 199, Humana Press, New Jersey, 2002 (Chapter 1).
- [43] M. Zaru, C. Sinico, A. Logu, C. Caddeo, F. Lai, M.L. Manca, A.M. Fadda, *J. Liposome Res.* 19 (2009) 68.
- [44] G. Dahms, *Cosmet. Toiletries* 101 (1986) 113.
- [45] S. Friberg, *J. Colloid Interface Sci.* 32 (1971) 49.
- [46] L. Brinon, S. Geiger, V. Alard, J.F. Tranchant, T. Pouget, G. Couarraze, *J. Soc. Cosmet. Chem.* 49 (1998) 1.
- [47] K. Klein, *Cosmet. Toiletries* 117 (2002) 30.
- [48] S. Singh, *Phys. Rep.* 324 (2000) 107.
- [49] M. Malmsten, *Surfactants and Polymers in Drug Delivery*, Drugs and the Pharmaceutical Sciences, Marcel Dekker, New York, 2002.
- [50] H.P. Klug, *X-ray Diffraction Procedures*, John Wiley & Sons, New York, 1954.
- [51] P. Holmqvist, P. Alexandridis, B. Lindman, *Macromolecules* 30 (1997) 6788.
- [52] Z.S. Németh, L. Halász, J. Pálkás, A. Bóta, T. Horányi, *Colloids Surf. A: Physicochem. Eng. Aspects* 145 (1998) 107.
- [53] T. Gao, J.M. Tien, Y.H. Choi, *Cosmet. Toiletries* 118 (2003) 41.
- [54] H. Wang, G. Zhang, Z. Du, Q. Li, W. Wang, D. Liu, X. Zhang, *J. Colloid Interface Sci.* 300 (2006) 348.
- [55] H.A. Barnes, J.F. Hutton, K. Walter, *An Introduction to Rheology*, Elsevier, New York, 1989.
- [56] M.L. Bruschi, D.S. Jones, H. Panzeri, M.P.D. Gremião, O. Freitas, E.H.G. Lara, *J. Pharm. Sci.* 96 (2007) 2074.
- [57] G.R. Leonardi, P.M.B.G. Maia Campos, *J. Cosmet. Sci.* 49 (1998) 23.
- [58] P.M.B.G. Maia Campos, G. Ricci, G.M. Silva, E.B. Santos, R.A. Lopes, M. Semprini, *J. Cosmet. Sci.* 50 (1999) 159.
- [59] N. Vucinić-Milanković, S. Savić, G. Vuleta, S. Vucinić, *Drug Dev. Ind. Pharm.* 33 (2007) 221.
- [60] J.H. Yang, Y.I. Kim, *Pharm. Res.* 4 (2002) 534.
- [61] P. Spiclin, M. Homar, A. Zupancic-Valant, M. Gasperlin, *Int. J. Pharm.* 256 (2003) 65.
- [62] C.N. Ellis, J.S. Weiss, T.A. Hamilton, J.T. Headington, A.S. Zelickson, *J. Voorhees, J. Am. Acad. Dermatol.* 23 (1990) 629.